

# Scavenging of DPPH by Persistent Free Radicals in Carbonized Particles

Karin H. Adolfsson,\* Ping Huang, Monika Golda-Cepa, Huan Xu, Andrzej Kotarba, and Minna Hakkarainen\*

Persistent free radicals (PFR) in carbonized particles may play a role in degradation of environmental compounds. The influence of PFR is evaluated in various carbonized particles on their radical scavenging efficiency upon the common radical indicator 2,2-diphenyl-1-picrylhydrazyl (DPPH). Carbonized particles are derived by hydrothermal carbonization of glucose (C-W) or glucose and urea (NC-W) and ionothermal carbonization of glucose and urea ionic liquid (IL) (NC-IL). The carbonized materials contain OH/COOH, C=C, and C-O functionalities. The addition of urea introduces NH/NH<sub>2</sub> functionalities. The content of polar surface groups is lower in IL-processed NC-IL. The scavenging ability, measured as DPPH UV-vis absorption decline, increases with concentration and time for all particles, while the efficiency changes are in the order of C-W > NC-W > NC-IL. Electron paramagnetic resonance analysis reveals similar radical concentration in all carbonized materials studied. The difference in efficiency is, thus, not directly related to the PFR concentration but rather to the type of PFR, surface functionalities and/or scavenging mechanism. According to the g-values, radicals in these particles are carbon-centered. The minor variation in g-values suggests interactions between the radicals and their environmental functional groups. This provides insights into the influence of PFR in carbonized materials on their radical scavenging efficiency.

## 1. Introduction

The radical scavenging capability of carbonized materials has been established in several works aiming for application in the biomedical and packaging fields among others.<sup>[1–9]</sup> Most of the applied carbonized materials consist of hydrothermally derived carbon dots and hydrochars. Hydrothermal carbonization (HTC) is a commonly applied method to produce carbonized materials from biomass.<sup>[10,11]</sup> The process is considered mild as it operates in water and at low temperatures (below 300 °C). During the process, the feed is transformed into carbonized particles by deoxygenation reactions.<sup>[12]</sup> Depending on the feed and process parameters, the properties of the carbonized particles may be tuned to some extent.<sup>[13]</sup> As an example, the addition of urea in the feed was shown to introduce nitrogen functionalities in the carbonized materials.<sup>[3]</sup>

The ionothermal carbonization (ITC) of biomass with ionic liquids (IL) as solvent is another method to produce carbonized materials.<sup>[14]</sup> IL are stable molten salts below 100 °C and considered green solvents due to their recyclability potential. There exist a wide variety of IL with organic cations and organic or inorganic anions, several of which solely or in combination with water have been applied for derivation of carbonized materials.<sup>[15–19]</sup> In general, the ITC-derived particles have been demonstrated to be similar to HTC particles, still, differences in for example porosities of the carbonized materials have been reported.<sup>[15]</sup> Furthermore, the use of imidazolium-based IL/water solvents in ITC processes instead of water was demonstrated to influence the amount of surface oxygen of the carbonized materials.<sup>[20,21]</sup>


For evaluating the scavenging efficiency of the aforementioned particles and other compounds, the nitrogen-centered radical 2,2-diphenyl-1-picrylhydrazyl (DPPH) is a commonly applied indicator.<sup>[22]</sup> The scavenging of DPPH radical can be quantified by UV-vis spectroscopy via monitoring the color transition, as the DPPH goes from a deep violet to yellow color in presence of a scavenging agent.<sup>[6]</sup> The scavenging ability of carbonized particles in case of DPPH has mainly been attributed to the hydrogen atom transfer (HAT)-mechanism.<sup>[1,3,6,7,23]</sup> It has been suggested that hydrogens are transferred from

K. H. Adolfsson, M. Hakkarainen  
Department of Fibre and Polymer Technology  
KTH Royal Institute of Technology  
Stockholm 100 44, Sweden  
E-mail: karinad@kth.se; minna@kth.se

P. Huang  
Department of Chemistry – Ångström Laboratory  
Uppsala University  
Box 523, Uppsala 751 20, Sweden

M. Golda-Cepa, A. Kotarba  
Faculty of Chemistry  
Jagiellonian University  
Krakow 30–387, Poland

H. Xu  
School of Materials Science and Physics  
China University of Mining and Technology  
Xuzhou 221116, P. R. China

 The ORCID identification number(s) for the author(s) of this article can be found under <https://doi.org/10.1002/adsu.202200425>.

© 2023 The Authors. Advanced Sustainable Systems published by Wiley-VCH GmbH. This is an open access article under the terms of the Creative Commons Attribution License, which permits use, distribution and reproduction in any medium, provided the original work is properly cited.

DOI: 10.1002/adsu.202200425

polar surface functionalities of the carbonized particles such as OH, COOH, NH<sub>2</sub>, and SH to DPPH radicals forming the neutral DPPH-H.

It has further been recognized that HTC particles contain persistent free radicals (PFR),<sup>[24]</sup> as mainly studied for carbonized materials derived under an oxygen-deficient atmosphere. It has further been shown that the PFR in carbonized materials take part in radical reactions. For instance, PFR were shown to be involved directly in the degradation of organic contaminants<sup>[24]</sup> or indirectly via the activation of other radicals.<sup>[25,26]</sup> With the help of electron paramagnetic resonance (EPR) spectroscopy, both concentration and type of PFR in carbonized materials can be determined.<sup>[27–29]</sup> Works related to HTC-derived carbon particles have been focusing on the correlation between type and concentration of PFR and production parameters such as type of biomass, temperature and time.

We hypothesized that the scavenging of DPPH by carbonized materials would be influenced by the presence of PFR. To enable a green production protocol of different carbonized materials, the renewable feed materials (glucose and urea) and solvents (water and imidazolium-based IL) were utilized in both HTC and ITC processes. The evaluation was focused on scavenging efficiency, the concentration and type of PFR between various carbonized particles.

## 2. Results and Discussion

Carbonaceous particles were derived from the renewable resources glucose and urea by utilizing water or ionic liquid (IL) AmimCl as solvents. The carbonized particles were evaluated for their capability to scavenge DPPH radical.

### 2.1. Characteristics of Carbonized Particles

The carbonized particles were produced in a microwave oven at 180 °C for 30 min. Glucose was used as feed for the derivation of the particles in water (C-W), while glucose and urea were utilized for production of the particles in water (NC-W) or in AmimCl IL (NC-IL). The scanning electron microscopy (SEM) images revealed that the water-processed C-W and NC-W were microsized spheres partly connected (Figure 1), which is a typical appearance of HTC particles.<sup>[30]</sup> This means that the addition of urea to glucose, for the derivation of NC-W, did not influence the morphology and size of the particles. When

AmimCl was utilized as a solvent for the preparation of NC-IL, flakelike and larger microsized particles were formed. In earlier reports, the use of IL as a solvent in similar processes have led to carbon materials with nanosized spherical particles and aerogels.<sup>[15,20]</sup> Complementary transmission electron microscopy (TEM) images of water (NC-W) and IL processed (NC-IL) materials further displayed the content of nanoparticles in the materials (Figure S2, Supporting Information). The mass yields of the derived C-W, NC-W and NC-IL were 15, 12 and 43%, respectively. Since the ITC process gave rise to a larger fraction of insolubles compared with the HTC processes, the detected variance could be due to different carbonization degrees<sup>[17,21]</sup> and the incorporation of IL in the particles.<sup>[14]</sup>

As revealed by Fourier transform infrared spectroscopy (FTIR), the obtained particles did not display sharp vibrational modes around 3000–3500 cm<sup>−1</sup> nor at lower frequencies region corresponding to the feed materials glucose and urea (Figure 2a). Instead, absorption bands reflecting different oxygen functionalities were present in the materials as is commonly encountered in HTC materials.<sup>[12]</sup> For all derived carbon particles, the functionalities O-H, C-H, C=O, C=C and C-O were located at 3200, 2910, 1770–1675, 1600–1554 and ≈1100 cm<sup>−1</sup>.<sup>[5]</sup> The C-O functionality at 1147 cm<sup>−1</sup> was most prominent in C-W and can be related to carboxylics. Another difference between the materials was the stretch mode referring to C=C-H located above 3000 cm<sup>−1</sup>, which was only noticed in the spectrum of NC-IL. This could be related to a higher degree of carbonization during ITC compared to HTC.<sup>[15]</sup> The HTC carbonization of biomass proceeds via saccharides to furan-based intermediates<sup>[13]</sup> and a similar reaction path has been suggested for ITC in IL.<sup>[19]</sup> The particles based on glucose and urea, NC-W and NC-IL, contained ≈10 times more nitrogen than the glucose-based C-W (Figure 2b). Whereas no significant difference in nitrogen content was detected between NC-W and NC-IL. The introduction of N-H functionalities has been suggested to occur when urea is utilized as feed in HTC processes.<sup>[3]</sup> The presence of amines/amides could be indicated by stretches of N-H above 3000 cm<sup>−1</sup> in the FTIR spectra but these absorption bands are overlapping with O-H.<sup>[5]</sup>

The produced particles were further analyzed with confocal Raman analysis (Figure 3). The D and G bands of the particles were detected at 1349–60 and 1592 cm<sup>−1</sup>, respectively. The D band corresponds to the breathing modes of C=C in rings and the G band to the in-plane bond stretching motion of C=C in rings and chains.<sup>[31]</sup> The intensity ratios of ID/IG were 0.5–0.6 for C-W and NC-W, whereas it was 0.9 for NC-IL. In

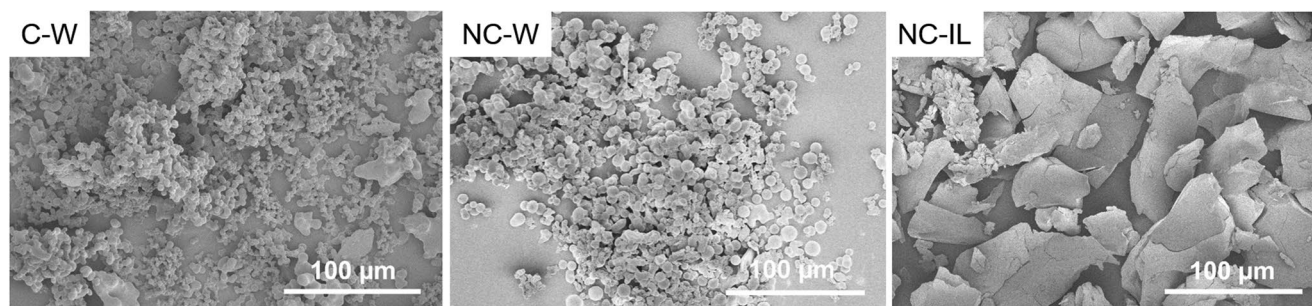


**Figure 1.** SEM images of C-W, NC-W and NC-IL.

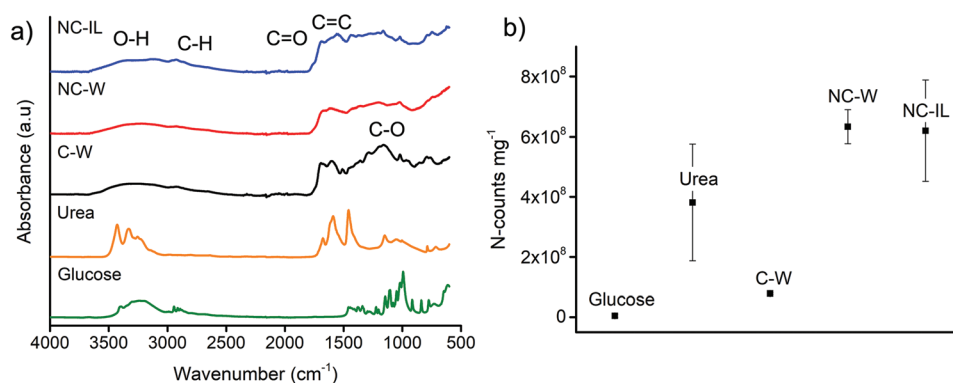


**Figure 2.** FTIR spectra a) and nitrogen analysis b) of carbonized particles and feed materials.

carbonized materials, the intensity ratio ID/IG is designated to the concentration of larger groups of aromatic rings.<sup>[32]</sup> For instance, it was shown that the ID/IG ratio became lower with higher temperature during carbonization as smaller groups of aromatics grew to larger structures.<sup>[21]</sup> In this work, the use of IL as solvent gave rise to the lower content of larger groups of aromatics in NC-IL compared to when using water for the derivation of C-W and NC-W. As earlier seen for both HTC<sup>[33]</sup> and ITC derived particles,<sup>[16]</sup> all particles had an amorphous character as visualized by the broad and flat peaks around  $2\theta = 22^\circ$  in the wide-angle X-ray diffraction (WAXD) spectra. The broad band is typically ascribed to the graphitic plane and was most noticeable for C-W.

Further chemical analysis was conducted with the surface analytical technique X-ray photoelectron spectroscopy (XPS) (Figure 4 and Table 1; Table S1, Supporting Information). Overall, the analysis was in agreement with the previous nitrogen analysis and detected the presence of nitrogen in NC-W and NC-IL. In addition, the water-processed particles C-W and NC-W had higher content of surface polar functionalities than the IL-processed particles NC-IL. As seen in high-resolution spectra of N 1s, the peak located between 399.8–400.6 eV translates to the content of the NH/NH<sub>2</sub> in both NC-W and NC-IL.<sup>[8]</sup> Notably the N/C ratio was higher for NC-W (0.11) than for NC-IL (0.05). This indicated that the nitrogen in NC-IL was mainly located in the bulk of the material, since previous nitrogen analysis showed comparable total nitrogen amounts in

NC-W and NC-IL. In the C 1s spectra, two peaks of C-W and NC-W located at 284.7 and 285.9 eV were attributed to C-C and C-O, respectively.<sup>[12]</sup> Whereas a sole peak of C-C functionality was displayed in NC-IL. This result was further reflected in the O/C ratios, which were 0.31 for C-W and NC-W, and significantly lower for NC-IL with a ratio of 0.11. Thus, the surface content of oxygen and nitrogen were higher for C-W and NC-W in comparison with NC-IL. The higher oxygen concentration on the surface of HTC-derived materials in comparison to the bulk has been attributed to the hydrolysis of already existing oxygen functionalities such as lactones and esters.<sup>[34]</sup> The two inequivalent peaks of the Cl 2p in NC-IL at 200.6 and 202.6 eV revealed the incorporation of organic Cl in the particles from AmimCl.<sup>[35]</sup> This could have contributed to the higher mass yield recorded for NC-IL.

The thermal stability and characteristics of the particles were evaluated with thermogravimetric analysis (TGA) (Figure 5). No significant differences in overall carbonization degree were observed between the particles, based on similar thermal stability over a temperature range from 300 to 600 °C. Carbonized materials generally display higher thermal stabilities than feed materials due to the greater carbon content.<sup>[36]</sup> The char yields were nearly 60% at a temperature of 600 °C. In comparison, the feed materials glucose and urea displayed char contents of 10–15% at the same temperature. The water-processed particles, C-W and NC-W, exhibited one clear decomposition step at 417 and 360 °C, respectively. Whereas the IL processed NCP-IL had

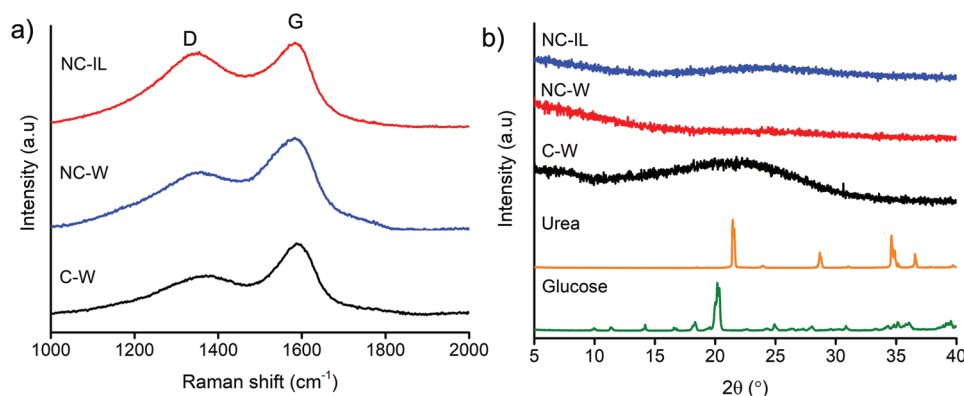


**Figure 3.** Confocal Raman spectra a) and WAXD spectra b) of carbonized particles and feed materials.

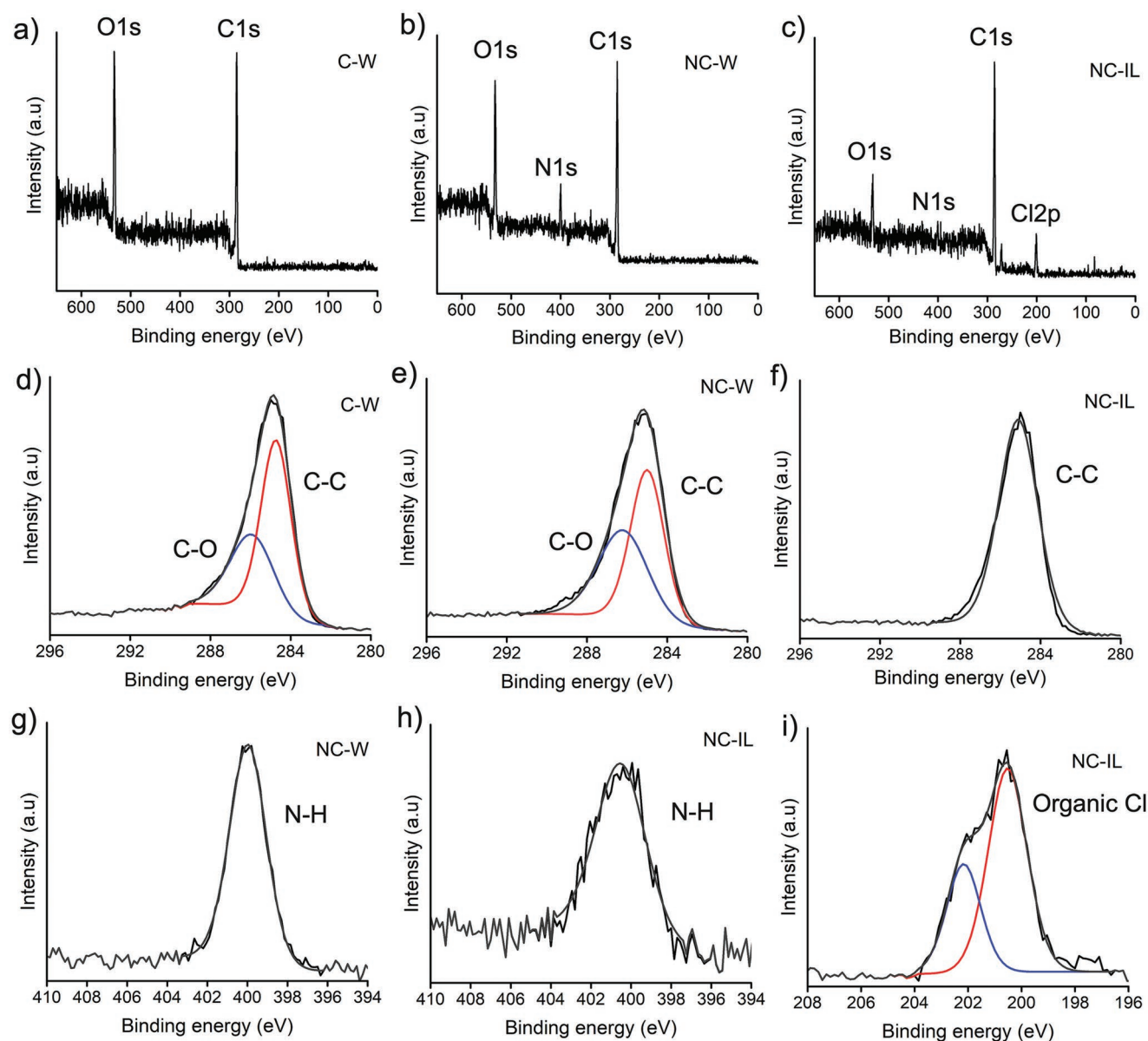


**Figure 4.** a–c) XPS survey spectra and d–f) C 1s high-resolution spectra of carbonized particles and g,h) N 1s high-resolution spectra of NC-W and NC-IL and i) Cl 2p high-resolution spectrum of NC-IL.

two decomposition steps at 300 and 423 °C. This indicates differences in chemical structures of all the particles, where the lower decomposition temperatures might be related to the presence of nitrogen functionalities.<sup>[37]</sup> All particles started to slowly decompose around 70 °C likely owing to the presence of low molecular weight compounds and water.

**Table 1.** At.% for the detected elements in different carbonized particles determined from XPS measurements.

At. %	C 1s	O 1s	N 1s	Cl 2p	O/C	N/C
C-W	76.1	23.8	–	–	0.31	–
NC-W	70.8	21.7	7.47	–	0.31	0.11
NC-IL	79.9	8.83	3.98	7.27	0.11	0.05

## 2.2. Scavenging Efficiency of Particles

The scavenging efficiency of the particles was evaluated toward DPPH radical in methanol dispersions using UV–vis spectroscopy. All carbonized particles displayed scavenging properties as shown in **Figure 6** and summarized in Table S2 (Supporting Information). It was shown that the scavenging efficiency of the particles increased with time (0.5–24 h) and concentration of particles (20–40 µg mL<sup>−1</sup>). After 30 min, CP-W displayed a scavenging efficiency of 70% at a concentration of 20 µg mL<sup>−1</sup>. At the same time and concentration, NC-W exhibited an efficiency of 42% and NC-IL had an efficiency of 13%. Thus, the efficiency decreased in the order of C-W, NC-W and NC-IL. These measured efficiencies toward DPPH radical were in a similar range to those of other HTC carbonized particles.<sup>[1]</sup> The scavenging



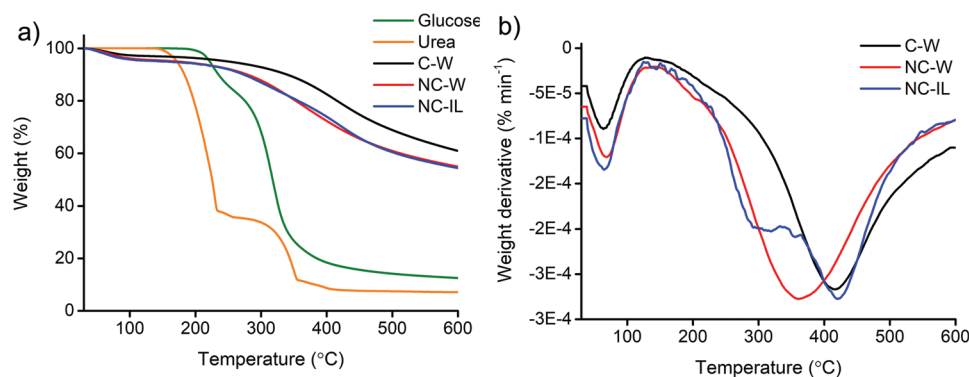


**Figure 5.** TG/DTA profiles of a) weight residue (%) and b) weight residue derivative ( $\% \text{ min}^{-1}$ ) of carbonized particles and feed materials.

of DPPH radical exerted by the particles was further shown to be time-dependent as earlier reported.<sup>[8]</sup> After 3 and 24 h, respectively, all particles displayed higher scavenging efficiency compared with the previously evaluated short time period, but with the same interrelated order of efficiency. When doubling the particle concentration to  $40 \mu\text{g mL}^{-1}$ , both C-W and NC-W, displayed increased efficiency of 100% already after 30 min. At the same time period, NC-IL had an efficiency of 27%, which was double the value recorded at  $20 \mu\text{g mL}^{-1}$ . The concentration dependency of carbonized particles on the scavenging efficiency of DPPH radical have been outlined in several other works.<sup>[1,3,8]</sup>

EPR measurements provided information about the radical concentration and type of radical species in the carbonized particles. The solid-state EPR analysis of all carbonized particles displayed a single but broadened signal (Figure 7). The determined EPR parameters: g-values, line width ( $\Delta B$ ) and spin concentration are summarized in Table 2. Spin counting revealed similar radical concentrations at a scale of  $10^9$  spins  $\text{mg}^{-1}$  for all carbonized particles. Hence, neither nitrogen doping nor solvent type in the preparation of the particles significantly influenced the radical concentration. This finding indicates that the different scavenging efficiencies, displayed among the particles with UV-vis, were not directly correlated to the radical concentration but rather to the type of species and/or the mechanism of scavenging. Confirming the UV-vis measurements, the characteristic peaks pattern originating from DPPH radical

vanished after contact with the particles in methanol dispersions (Figures S7 and S8, Supporting Information). In case of NC-IL the DPPH peak intensities were reduced but still present, which may be due to the lower scavenging efficiency of NC-IL.

Since the type of radical species could influence the scavenging efficiencies, the g-values of carbonized particles were recorded in solid-state. The g-values of the particles were shown to be within the range of 2.0035–2.0040 (Table 2). Radicals in the C-W and the NC-IL displayed g-value similarity attributed to carbon-centered species.<sup>[29]</sup> Meanwhile, NC-W showed a slightly higher g-value, indicating an adjacent oxygen atom to the carbon radical.<sup>[24]</sup> Other detected differences in g-factors between the particles, although all carbon-centered, are most likely a result of various chemicals environment containing nitrogen in NC-W, and nitrogen and chloride in NC-IL. The different surface functionalities of the particles as outlined with chemical analysis indicated that C-W and NC-W may have interacted more strongly with DPPH radicals in comparison to NC-IL, or differences in solubility in methanol, leading to higher scavenging efficiency.<sup>[23]</sup> Furthermore, the fact that NC-IL displayed significantly lower scavenging efficiency in comparison with the other particles suggests a different

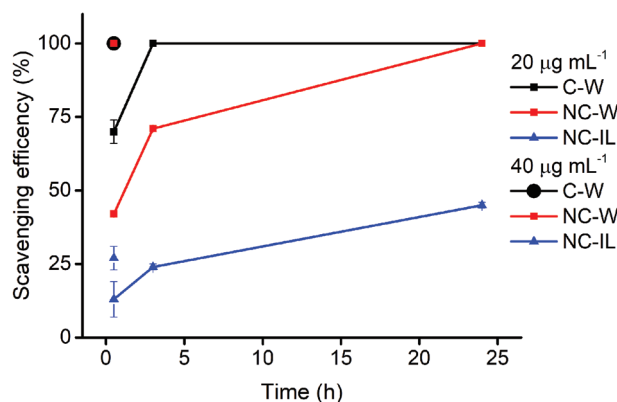


**Figure 6.** Scavenging efficiency of carbonized particles as determined by UV-vis measurements in presence of DPPH radical in methanol at the wavelength of 517 nm.

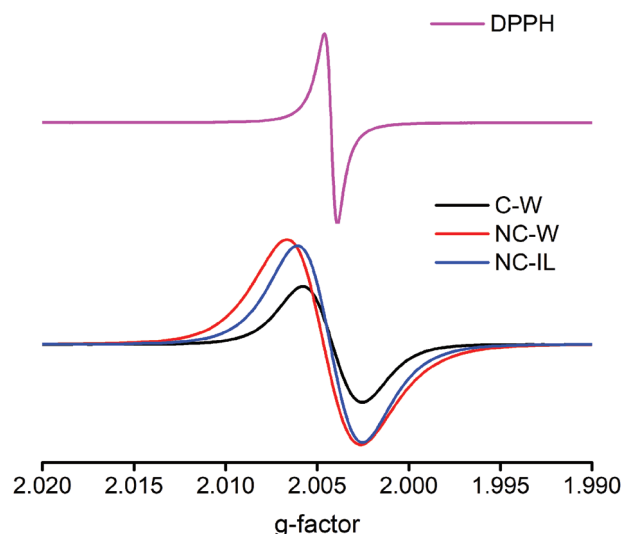


**Figure 7.** EPR spectra of carbonized particles in solid state.

**Table 2.** EPR values in g-factor, line width ( $\Delta B$ ) and spin concentration of the carbonized materials.

Solid-state	g-factor	$\Delta B$ [mT]	Concentration [spins $\text{mg}^{-1}$ ]	Line shape
C-W	2.0035	0.570	$\approx 5 \times 10^9$	Gaussian
NC-W	2.0040	0.698	$\approx 12 \times 10^9$	Gaussian+Lorentzian
NC-IL	2.0036	0.624	$\approx 4 \times 10^9$	Gaussian

scavenging mechanism, which should be further investigated in future study.

### 3. Conclusion

Persistent free radicals (PFR) in carbonized particles were evaluated for scavenging of the DPPH radical. The water-processed C-W, based on glucose, and NC-W based on glucose and urea, consisted of microsized spherical particles. The IL (AmimCl) processed NC-IL, based on glucose and urea, were larger microsized flakelike particles. All the prepared carbonaceous particles contained COOH/OH, C=O, C=C, and C-O functionalities. With the addition of urea in the feeds, NH/NH<sub>2</sub> functional groups were additionally introduced into NC-W and NC-IL. The concentration of the surface polar oxygen and nitrogen-containing groups were lower in NC-IL compared to those of C-W and NC-W. UV-vis spectroscopy revealed increased scavenging efficiency of all particles toward the DPPH radical with both concentration and time. The efficiency was in the order of C-W > NC-W > NC-IL, where the scavenging efficiency detected for NC-IL was considerably lower than that for C-W and NC-W. EPR analysis showed that the spin concentration of the carbonized particles was in similar range, and hence did not correlate with their scavenging efficiencies. The g-values of PFR in all the investigated particles corresponded to carbon-centered radical species, but with small differences attributed to the presence of adjacent oxygen in NC-W, as well as the content of nitrogen and chloride from material preparations. This effort provides insights into the scavenging exerted by PFR in carbonized materials, where the findings suggest influence from the type of PFR, surface functionalities and/or another scavenging mechanism on their radical scavenging efficiencies.

### 4. Experimental Section

**Materials and Chemicals:** Glucose, urea, allyl chloride, and 1-methylimidazolium were purchased from Sigma-Aldrich. 2,2-diphenyl-1-picrylhydrazyl (DPPH) and dimethyl sulfoxide (DMSO-*d*<sub>6</sub>; 99.9%) were purchased from TCI Cambridge Isotope Laboratories, Inc. Methanol (98.5%) was procured from VWR. All chemicals were used as received.

**Synthesis of Ionic Liquid:** 1-methyl, 3-allylimidazoliu chloride (AmimCl) was synthesized according to the previously reported procedure.<sup>[38,39]</sup> 1-methylimidazole (32 mL, 0.4 mol, 1.0 equiv) was added in a round-bottom flask equipped with a magnetic stirrer, where after allyl chloride (41 mL, 0.5 mol, 1.25 equiv) was added slowly under stirring at RT. The reaction was heated to 55 °C for 18–24 h with a reflux condenser equipped with a CaCl<sub>2</sub> tube. Excess allyl chloride was removed with a rotary evaporator. If unreacted 1-methylimidazole remained, it was extracted with ethyl acetate. The AmimCl was stored in a vacuum oven.

**Carbonization Processes:** Glucose (2 g) was added into a pressure-controlled vessel with 20 mL of deionized water, which was placed in a microwave oven (Milestone Inc.). The temperature was increased to 180 °C with a ramp time of 5 min and left to run for 25 min with stirring inside the vessel. After cooling to room temperature, the condensed phase was collected through centrifugation (5000 rpm, 5 min) as precipitate and washed with deionized water. The collected particles were named C-W. The same procedure was used for the production of nitrogen-doped carbonized particles but with the feed materials glucose (1.8 g) and urea (0.2 g), and with water or AmimCl as solvent. The particles were named NC-W and NC-IL based on the use of water or AmimCl, respectively, as reaction medium. AmimCl was collected after the production of NC-IL and analyzed with nuclear magnetic resonance (<sup>1</sup>H-NMR) displaying recyclability possibilities (Figure S1, Supporting Information).

**Characterization Methods:** Fourier transform infrared spectroscopy (FTIR) analysis was performed at a resolution of 4 cm<sup>-1</sup> on the instrument PerkinElmer Spectrum 100 with an ATR crystal accessory. Confocal Raman spectroscopy analyses were acquired on an HR800 UV Jobin Yvon Raman combined with a solid-state laser utilizing a lambda excitation ( $\lambda_{\text{ex}}$ ) of 514 nm. PANalytical X'Pert PRO diffractometer equipped with a silica monocrystal sample holder was used for the wide-angle X-ray diffraction (WAXD) analysis. Cu K $\alpha$  ( $\lambda = 1.541874$  nm) was operating at a voltage of 45 kV and a current of 40 mA. Nuclear magnetic resonance (<sup>1</sup>H-NMR) spectra of AmimCl before and after production of NC-IL were recorded on Bruker Advance 400 MHz spectrometer in DMSO-*d*<sub>6</sub> at room temperature.

For the X-ray photoelectron spectra, the SESR4000 analyzer (Gammadata Scientia), equipped with the monochromatic Al K $\alpha$  X-ray source (1486.6 eV) operated at 250 W with a pass energy of 100 eV for the survey and narrow scans. The base pressure in the UHV chamber was below  $5 \times 10^{-9}$  mbar. The analysis of collected spectra was performed with the use of CasaXPS Version 2.3.18PR1.0. The electron binding energy of the Cls peak was referenced at 285 eV.

Electron paramagnetic resonance (EPR) spectroscopy analysis was performed on a Bruker EMX-micro spectrometer equipped with an EMX-Primum bridge and an ER4119HS resonator. Powder samples were loaded into capillary tubes (i.d. 0.75 mm), sealed with playdoh and weighed before EPR examination. Solution samples were prepared in Eppendorf tubes, by transferring 200  $\mu\text{L}$  DPPH solution from a pre-prepared stock solution made of DPPH powder at the tip of a spatula dissolved in MeOH into Eppendorf tubes. A PFR powder sample at tip of a spatula was added into the DPPH. Then the solution mixture was subsequently vortexed, centrifuged and loaded to a capillary tube, sealed with playdoh and inserted into a normal EPR tube before EPR reading. EPR spectral recording settings were: microwave frequency, 9.878 GHz; microwave power, 40  $\mu\text{W}$  for solid samples and 10 mW for solution samples; modulation frequency, 100 kHz; modulation amplitude 0.3 mT. The Xep software package (Bruker) was used for data acquisition and processing of spectra.

Thermogravimetric analysis (TGA) was performed with Mettler-Toledo (TGA)/SDTA 851. A total of 4–5 mg of each sample was placed into a 70  $\mu\text{L}$  alumina cup including in all cases a replicate of 2 samples. The samples were heated at a rate of 10 °C min<sup>-1</sup> from 30 to 700 °C with an N<sub>2</sub> flow rate of 50 mL min<sup>-1</sup>. An ANTEK 700 nitrogen analyzer was used for determining the average nitrogen counts mg<sup>-1</sup> of the samples. Each sample was analyzed 2–3 times with a weight of 1–3 mg per sample. Scanning electron microscopy (SEM) images were acquired on an ultrahigh-resolution FE-SEM Hitachi S-4800. The samples were coated with a 3–5 nm Pt/Pd layer prior analysis. Transmission electron microscopy (TEM, FEI, USA) images were recorded of NCP-W and NCP-IL using an accelerating voltage of 80 kV. The methanol dispersions (0.2 mg mL<sup>-1</sup>) were first bath sonicated for 30 min, and then the supernatants were drop casted on the grid.

**Evaluation of Scavenging Efficiency:** The scavenging efficiency of the particles was evaluated toward the DPPH radical (100  $\mu\text{M}$ ) in methanol. First, the obtained carbonized particles C-W, NC-W, and NC-IL were prepared in a methanol dispersion (200  $\mu\text{g mL}^{-1}$ ) and bath sonicated

for 30 min. Thereafter, the supernatants of the particle dispersions were collected through centrifugation (5000 rpm, 5 min). The dispersions of particles (40 or 80  $\mu\text{g mL}^{-1}$ ) and a DPPH radical methanol solution were mixed in equal volume (in total 3 mL), where after their scavenging efficiency (%) was evaluated with UV-vis spectroscopy (Shimadzu UV-2550) after 0.5, 3 and 24 h  $\pm$  5 min. The scavenging efficiencies of the dispersions were assessed at a wavelength 517 nm, where the absorption and scattering of the carbonaceous particles is low (see Figure S4, Supporting Information) and calculated according to (Equation 1).

$$\text{Scavenging efficiency(\%)} = \frac{(A_{0,t} - A_{t,t})}{A_{0,t}} \times 100 \quad (1)$$

where  $A_{0,t}$  is the absorbance of DPPH radical at the time  $t$  and  $A_{t,t}$  is the concentration of the dispersions with particles and DPPH radical at time  $t$ .

## Supporting Information

Supporting Information is available from the Wiley Online Library or from the author.

## Acknowledgements

Åforsk foundation (grant no. 20–333) is acknowledged for financial support.

## Conflict of Interest

The authors declare no conflict of interest.

## Data Availability Statement

The data that support the findings of this study are available in the supplementary material of this article.

## Keywords

carbonized particles, hydrothermal, ionothermal, persistent free radicals, scavenging of DPPH

Received: October 5, 2022

Revised: December 29, 2022

Published online: January 22, 2023

- [1] W. Zhang, J. Chavez, Z. Zeng, B. Bloom, A. Sheardy, Z. Ji, Z. Yin, D. H. Waldeck, Z. Jia, J. Wei, *ACS Appl. Nano Mater.* **2018**, 1, 2699.
- [2] M. Gimenez, M. Rodríguez, L. Montoro, F. Sardella, G. Rodríguez-Gutierrez, P. Monetta, C. Deiana, *Biomass Bioenerg.* **2020**, 143, 105875.
- [3] W. Zhang, Z. Zeng, J. Wei, *J. Phys. Chem. C* **2017**, 121, 18635.
- [4] K. kanthi Gudimella, G. Gedda, P. S. Kumar, B. K. Babu, B. Yamajala, B. V. Rao, P. P. Singh, D. Kumar, A. Sharma, *Environ. Res.* **2022**, 204, 111854.

- [5] A. Sachdev, P. Gopinath, *Analyst* **2015**, 140, 4260.
- [6] P. Das, S. Ganguly, S. Margel, A. Gedanken, *Langmuir* **2021**, 37, 3508.
- [7] C. Murru, R. Badía-Lañón, M. E. Díaz-García, *Antioxidants* **2020**, 9, 1459.
- [8] S. Huangfu, G. Jin, Q. Sun, L. Li, P. Yu, R. Wang, L. Zhang, *Polym. Degrad. Stab.* **2021**, 186, 109506.
- [9] D. Licursi, C. Antonetti, M. Mattonai, L. Pérez-Armada, S. Rivas, E. Ribechini, A. M. R. Galletti, *Ind. Crops Prod.* **2018**, 112, 6.
- [10] K. H. Adolfsson, N. Yadav, M. Hakkarainen, *Curr Opin Green Sustain Chem* **2020**, 23, 18.
- [11] Z. Feng, K. H. Adolfsson, Y. Xu, H. Fang, M. Hakkarainen, M. Wu, *Sustain. Mater. Technol.* **2021**, 29, e00304.
- [12] M. Sevilla, A. B. Fuertes, *Carbon N Y* **2009**, 47, 2281.
- [13] S. A. Nicolae, H. Au, P. Modugno, H. Luo, A. E. Szego, M. Qiao, L. Li, W. Yin, H. J. Heeres, N. Berge, M.-M. Titirici, *Green Chem.* **2020**, 22, 4747.
- [14] Z. Xie, D. S. Su, *Eur. J. Inorg. Chem.* **2015**, 1137.
- [15] Z. L. Xie, R. J. White, J. Weber, A. Taubert, M. M. Titirici, *J. Mater. Chem.* **2011**, 21, 7434.
- [16] P. Zhang, J. Yuan, T.-P. Feller, M. Antonietti, H. Li, Y. Wang, *Angew. Chem., Int. Ed.* **2013**, 52, 6028.
- [17] L. Cibien, M. Parot, P. N. Fotsing, P. Gaveau, E. D. Woumfo, J. Vieillard, A. Napoli, N. Brun, *Green Chem.* **2020**, 22, 5423.
- [18] L. L. Ma, W. J. Liu, X. Hu, P. K. S. Lam, J. R. Zeng, H. Q. Yu, *Chem. Eng. J.* **2020**, 400, 125969.
- [19] J. S. Lee, R. T. Mayes, H. Luo, S. Dai, *Carbon N Y* **2010**, 48, 3364.
- [20] H. Yang, X. Cui, Y. Deng, F. Shi, *J. Mater. Chem.* **2012**, 22, 21852.
- [21] Z. Huang, L. Shi, Y. Muhammad, L. Li, *J. Colloid Interface Sci.* **2021**, 586, 423.
- [22] J. D. Yeo, F. Shahidi, *J. Agric. Food Chem.* **2019**, 67, 7526.
- [23] P. Ezati, J. W. Rhim, R. Molaei, R. Priyadarshi, S. Roy, S. Min, Y. H. Kim, S. G. Lee, S. Han, *Sustain. Mater. Technol.* **2022**, 32, e00397.
- [24] Y. Qin, G. Li, Y. Gao, L. Zhang, Y. S. Ok, T. An, *Water Res.* **2018**, 137, 130.
- [25] J. Yu, Z. Zhu, H. Zhang, X. Shen, Y. Qiu, D. Yin, S. Wang, *Chem. Eng. J.* **2020**, 398, 125538.
- [26] G. Fang, J. Gao, C. Liu, D. D. Dionysiou, Y. Wang, D. Zhou, *Environ. Sci. Technol.* **2014**, 48, 1902.
- [27] Y. Zhu, J. Wei, Y. Liu, X. Liu, J. Li, J. Zhang, *Sci. Rep.* **2019**, 9, 17092.
- [28] P. Gao, D. Yao, Y. Qian, S. Zhong, L. Zhang, G. Xue, H. Jia, *Environ. Chem. Lett.* **2018**, 16, 1463.
- [29] A. Trubetskaya, P. A. Jensen, A. D. Jensen, P. Glarborg, F. H. Larsen, M. L. Andersen, *Biomass Bioenergy* **2016**, 94, 117.
- [30] C. Falco, N. Bacille, M.-M. Titirici, *Green Chem.* **2011**, 13, 3273.
- [31] A. C. Ferrari, *Solid State Commun.* **2007**, 143, 47.
- [32] D. M. Keown, X. Li, J.-I. Hayashi, C. Z. Li, *Fuel Process. Technol.* **2008**, 89, 1429.
- [33] K. H. Adolfsson, M. Golda-Cepa, N. B. Erdal, J. Duch, A. Kotarba, M. Hakkarainen, *Adv Sustain Syst* **2019**, 3, 1800148.
- [34] S. Reiche, R. Blume, X. C. Zhao, D. Su, E. Kunkes, M. Behrens, R. Schlögl, *Carbon N Y* **2014**, 77, 175.
- [35] U. Dettlaff-Weglikowska, V. Skákalová, R. Graupner, S. H. Jhang, B. H. Kim, H. J. Lee, L. Ley, Y. W. Park, S. Berber, D. Tománek, S. Roth, *J. Am. Chem. Soc.* **2005**, 127, 5125.
- [36] S. Poomsawat, W. Poomsawat, *Case Stud. Therm. Eng.* **2021**, 27, 101255.
- [37] M.-M. Titirici, A. Thomas, M. Antonietti, *J. Mater. Chem.* **2007**, 17, 3412.
- [38] H. Zhang, J. Wu, J. Zhang, J. He, *Macromolecules* **2005**, 38, 8272.
- [39] L. H. Gustavsson, K. H. Adolfsson, M. Hakkarainen, *Biomacromolecules* **2020**, 21, 1752.